F^- coordination environments around Eu^{3+} and Er^{3+} in MF_n-BaF_2-LnF_3 glasses (M = Zn, Al, Ga, Sc, Zr or Hf; *n* = **2**, 3 or 4; Ln = Eu or Er)

1998 J. Phys.: Condens. Matter 10 9711

(http://iopscience.iop.org/0953-8984/10/43/014)

J. Phys.: Condens. Matter **10** (1998) 9711–9720. Printed in the UK PII: S0953-8984(98)95487-X

F^- coordination environments around Eu^{3+} and Er^{3+} in MF_n–BaF_2–LnF_3 glasses (M = Zn, Al, Ga, Sc, Zr or Hf; n = 2, 3 or 4; Ln = Eu or Er)

Y Kawamoto†, K Ogura†, M Shojiya†, M Takahashi† and K Kadono‡

† Department of Chemistry, Faculty of Science, Kobe University, Nada, Kobe 657-8501, Japan
‡ Department of Optical Materials, Osaka National Research Institute, AIST, Ikeda, Osaka 563-8577, Japan

Received 30 June 1998, in final form 20 August 1998

Abstract. The F^- coordination environments around Eu^{3+} and Er^{3+} in MF_n–BaF_2–LnF_3 glasses (M = Zn, Al, Ga, Sc, Zr or Hf; n = 2 for Zn, 3 for Al, Ga and Sc and 4 for Zr and Hf; Ln = Eu or Er) were examined by Eu-L_{III} and Er-L_{III} EXAFS spectroscopy and by Eu^{3+} emission spectroscopy. The EXAFS analysis revealed that Eu^{3+} and Er^{3+} in each glass system have almost the same F^- coordination environments except for a slight difference due to lanthanoid contraction and also that the F^- coordination environments around Eu^{3+} and Er^{3+} significantly vary with the MF_n glass system. The latter result was also confirmed by Eu^{3+} emission spectra of the respective glass systems. The present study gave experimental evidence for the validity of the use of Eu^{3+} instead of Er^{3+} in order to examine the physicochemical environments of Er^{3+} in fluoride glasses.

1. Introduction

At present, rare earth-doped fluoride glasses have received much attention as a variety of photonics materials. As rare earth ions, for example, there are La^{3+} and Gd^{3+} for optical fibres with ultra-low transmission losses, Nd^{3+} for fibre lasers, Pr^{3+} for fibre amplifiers, Eu^{2+} and Sm^{2+} for photochemical hole burning memory devices and Nd^{3+}, Ho^{3+}, Er^{3+} and Tm^{3+} for infrared to visible upconversion luminescence devices [1].

Among these photonics materials, upconversion luminescence devices have received a great deal of interest because of the possibility of infrared-pumped visible lasers. Therefore a number of studies have been carried out on upconversion luminescence characteristics in fluoride glasses. In particular, heavy metal fluoride glasses such as ZrF_4-, HfF_4- and ThF_4-based glasses are considered to be the best candidate as host glasses for generating upconversion luminescence of high emission efficiency. Thus the Er^{3+} upconversion luminescence characteristics have been examined on fluorozirconate [2], fluorohafnate [3] and fluorothornate [4] glasses. Besides the ZrF_4-, HfF_4- and ThF_4-based glasses, the ZnF_2-, CdF_2-, AlF_3-, GaF_3-, InF_3- and ScF_3-based glasses have also been considered as glass hosts. The Er^{3+} upconversion luminescence characteristics in these glasses have been examined in detail [5, 6]. In these studies, Eu^{3+} is employed as a probe of Er^{3+} to analyse physicochemical environments of Er^{3+} [2, 5–8]. However there is no experimental evidence for the validity of the replacement of Eu^{3+} for Er^{3+} in order to examine the physicochemical environments of Er^{3+}. The object of the present study is to examine the validity of the replacement of Eu^{3+} for Er^{3+}.

0953-8984/98/439711+10$19.50

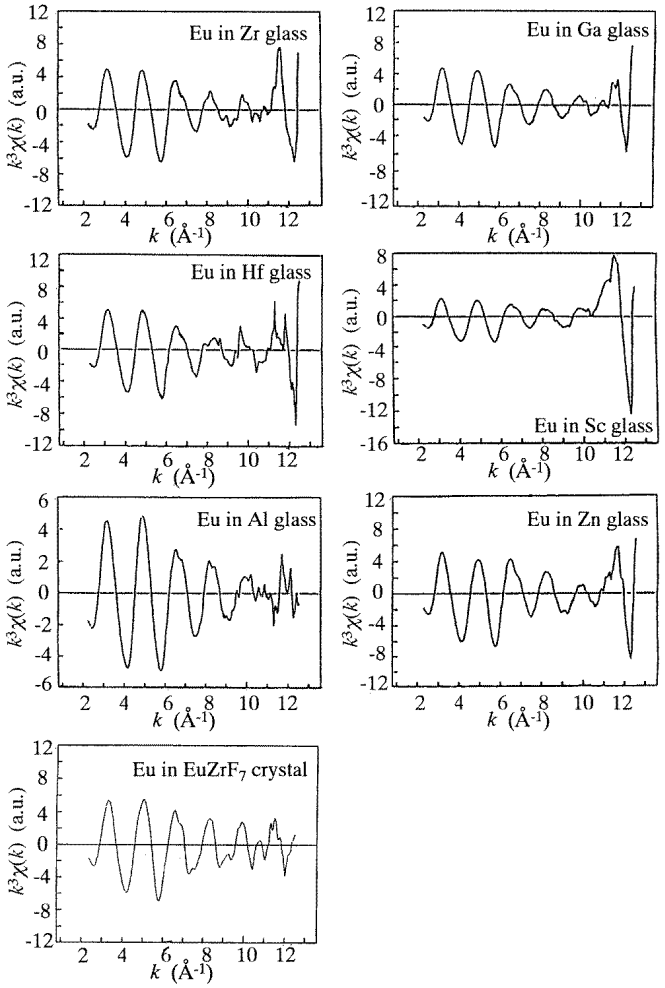

Figure 1. Eu-L_{III} and Er-L_{III} EXAFS oscillation, $k^3\chi(k)$, curves of the Zn, Al, Ga, Sc, Zr and Hf glasses and the $EuZrF_7$ and $ErZrF_7$ crystals.

In this study the F^- coordination environments around Eu^{3+} and Er^{3+} in fluoride glasses are investigated on ZnF_2-, AlF_3-, GaF_3-, ScF_3-, ZrF_4- and HfF_4-based glasses by Eu^{3+} and Er^{3+} EXAFS spectroscopy and Eu^{3+} emission spectroscopy.

2. Experimental procedure

2.1. Sample preparation

For the purpose of the present study it is desirable that glass samples for ZnF_2-, AlF_3-, GaF_3-, ScF_3-, ZrF_4- and HfF_4-based glass systems have the same composition. Unfortunately, however, glasses of the same composition could not be obtained because of differences in glass-forming tendency in each glass system. Therefore, glasses whose compositions are as close as possible were adopted. The compositions of the prepared

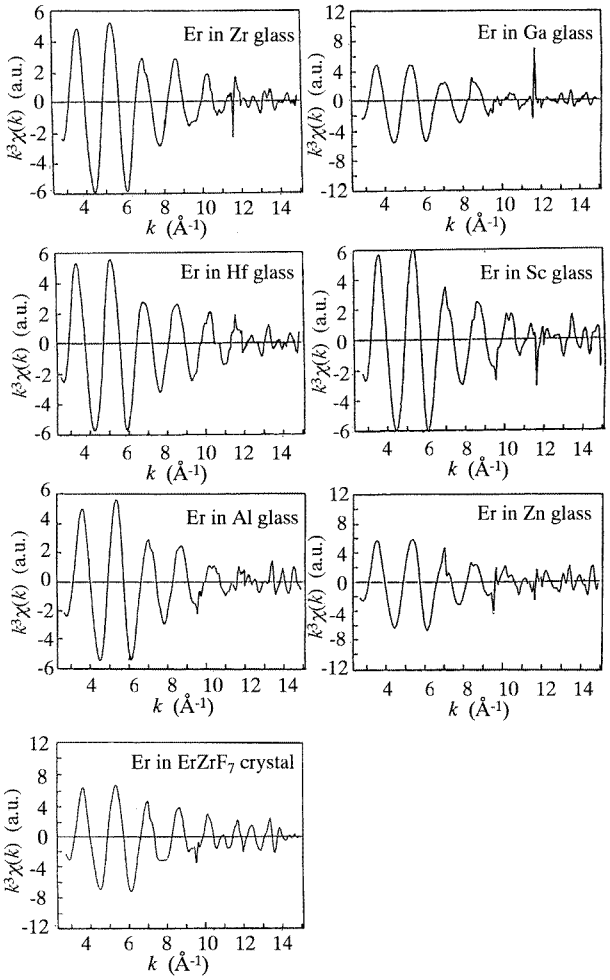

Figure 1. (Continued)

glasses are $55ZnF_2 \cdot 30BaF_2 \cdot 15LnF_3$, $45AlF_3 \cdot 30BaF_2 \cdot 25LnF_3$, $45GaF_3 \cdot 30BaF_2 \cdot 25LnF_3$, $45ScF_3 \cdot 40BaF_2 \cdot 15LnF_3$, $50ZrF_4 \cdot 30BaF_2 \cdot 20LnF_3$ and $50HfF_4 \cdot 30BaF_2 \cdot 20LnF_3$ (Ln = Eu or Er). Hereafter these glasses are abbreviated as the Zn, Al, Ga, Sc, Zr and Hf glasses, respectively. The procedure of glass preparation is described elsewhere [5].

Crystalline $EuZrF_7$ and $ErZrF_7$ were prepared as reference specimens in EXAFS experiments according to a procedure described in the literature [9]. In the sample preparation, guaranteed reagent grade chemicals of EuF_3, ErF_3 and ZrF_4 were used as the raw materials. The synthesized crystals were identified to be the single phases by x-ray powder diffraction measurements.

2.2. Eu and Er EXAFS measurements

For EXAFS measurements the prepared Zn, Al, Ga, Sc, Zr and Hf glasses and the synthesized $EuZrF_7$ and $ErZrF_7$ crystals were finely powdered under an Ar atmosphere in a glove box and pressed into thin discs with polyethylene powder.

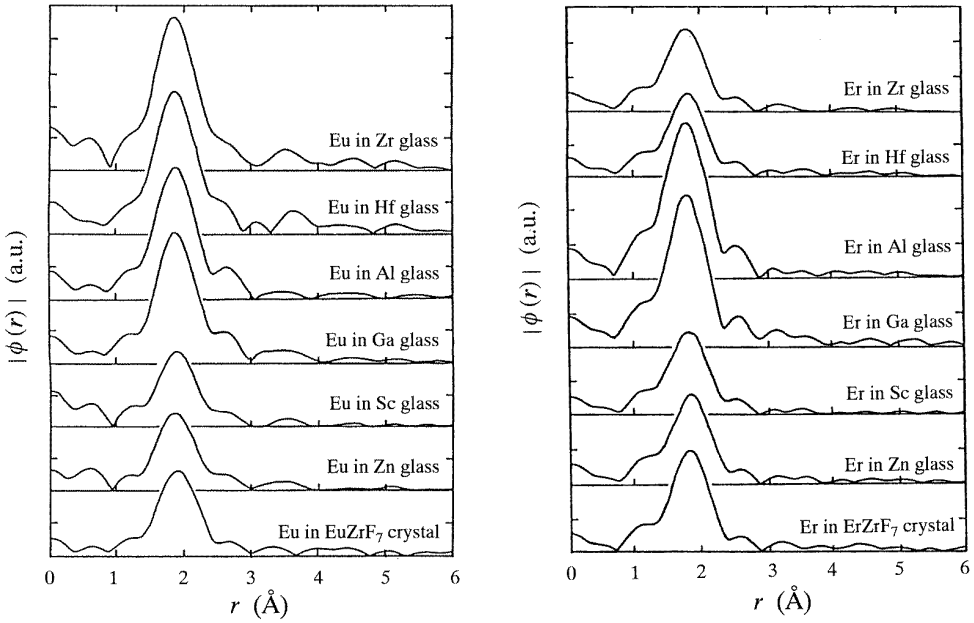

Figure 2. Fourier transform magnitude, $|\phi(r)|$, curves obtained for the Zn, Al, Ga, Sc, Zr and Hf glasses and the $EuZrF_7$ and $ErZrF_7$ crystals.

EXAFS measurements were carried out at the EXAFS facilities (BL-7C) at the Photon Factory in The National Laboratory for High Energy Physics. The positron energy and the ring current of the storage ring were 2.5 GeV and 200–360 mA, respectively. A monochromator with two flat Si(111) ($d = 3.1355$ Å) was used. The incident beam intensity of x-rays, I_0, and the transmitted beam intensity through samples, I, were monitored by ionization chambers (17 and 31 cm in length) with flowing gases of 100% N_2 and 75% $N_2 + 25\%$ Ar, respectively. The EXAFS measurements were made at ambient temperature. The Eu-L_{III} and Er-L_{III} absorption data were collected in the energy range from 1000 eV on the low energy side of the Eu-L_{III} and Er-L_{III} absorption edges (7.00 and 8.36 keV, respectively) to about 1200 eV on the high energy side. In order to obtain the Fourier transform magnitude, $|\phi(r)|$, from the EXAFS oscillation, EXAFS analysis was performed according to the Teo procedure [10]. In the extraction of the EXAFS oscillation from absorption spectra, the background absorption was calculated by employing the Victreen formula extrapolation, and the smooth Eu-L_{III} and Er-L_{III} shell absorption due to isolated Eu and Er atoms was estimated by using an iterative smoothing method. The energies of the absorption edges for Eu-L_{III} and Er-L_{III} were taken as 7000 and 8360 eV, respectively, and the EXAFS oscillation was converted into k-space to obtain $\chi(k)$.

2.3. Measurements of Eu^{3+} emission spectra

The emission spectra of the $^5D_0 \rightarrow {}^7F_J$ ($J = 0$, 1 and 2) transition of Eu^{3+} in the Zn, Al, Ga, Sc, Zr and Hf glasses were measured in the wavelength range 560–640 nm with a fluorescence spectrophotometer (Hitachi 850) at room temperature, using 395 nm light of an Xe lamp as the excitation source.

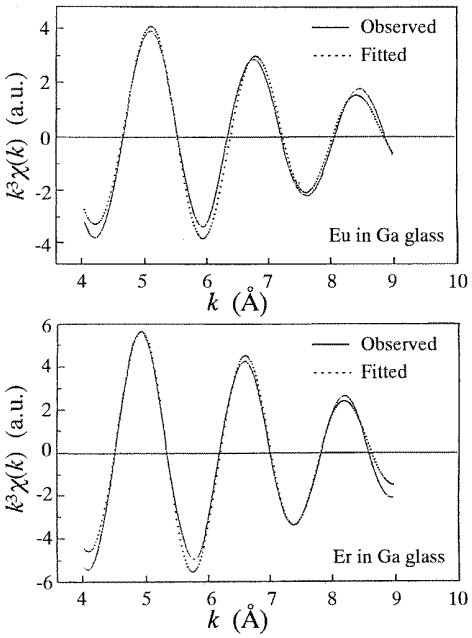

Figure 3. Curve fitting of $k^3\chi(k)$ for Eu^{3+} and Er^{3+} in the Sc glass.

3. Results

3.1. Eu and Er EXAFS analyses

The Eu-L_{III} and Er-L_{III} EXAFS oscillations, $k^3\chi(k)$, of the Zn, Al, Ga, Sc, Zr and Hf glasses and the $EuZrF_7$ and $ErZrF_7$ crystals are shown in figure 1. The $k^3\chi(k)$ curves were analysed by using an XABSGRX1 program cited in [11, 12]. Fourier transformation of $k^3\chi(k)$ was performed in the k range of 3.0 to 10.0 $Å^{-1}$ to obtain the Fourier transform magnitude, $|\phi(r)|$. The $|\phi(r)|$ curves obtained for the Zn, Al, Ga, Sc, Zr and Hf glasses and the $EuZrF_7$ and $ErZrF_7$ crystals are shown in figure 2. Fourier backfiltering was conducted in the k range of 1.0 to 2.4 Å. The phase shift and backscattering amplitude values which are necessary in performing curve fitting were obtained by using the $EuZrF_7$ and $ErZrF_7$ crystals as reference specimens. The F^- coordination numbers of Eu^{3+} and Er^{3+} in the $EuZrF_7$ and $ErZrF_7$ crystals were taken as eight because all the rare-earth fluorozirconates $LnZrF_7$ (Ln = rare earth) are isotypes, and Sm^{3+} in the $SmZrF_7$ crystal are surrounded by 8 F^- [9]. On the other hand, the Eu^{3+}–F^- and Er^{3+}–F^- interionic distances were taken as 2.396 and 2.334 Å, respectively, based on the effective ionic radii of Eu^{3+} (1.066 Å), Er^{3+} (1.004 Å) and F^- (1.33 Å) [13]. Curve fitting of $k^3\chi(k)$ was performed in the k range of 4.0 to 9.0 $Å^{-1}$ to obtain the Eu^{3+}–F^- and Er^{3+}–F^- interionic distances and the F^- coordination numbers around Eu^{3+} and Er^{3+}. An example of curve fitting for Eu^{3+} and Er^{3+} in the Sc glass is shown in figure 3.

The Eu^{3+}–F^- and Er^{3+}–F^- interionic distance, F^- coordination number and Debye–Waller factor values obtained for Eu^{3+} and Er^{3+} in the Zn, Al, Ga, Sc, Zr and Hf glasses are summarized in table 1. Experimental errors in interatomic distance and coordination number were estimated by performing the EXAFS measurement of the Al glass several times.

Table 1. Interionic distances, r_{Eu-F} and r_{Er-F}, F^- coordination numbers, $CN_F(Eu)$ and $CN_F(Er)$, and Debye–Waller factors, σ, obtained for the Eu^{3+}–F^- and Er^{3+}–F^- pairs in the Zn, Al, Ga, Sc, Zr and Hf glasses.

Glass	r_{Eu-F} (Å)	$CN_F(Eu)$	σ(Å^2)	r_{Er-F} (Å)	$CN_F(Er)$	σ(Å^2)
Zn	2.365 ± 0.005	7.58 ± 0.75	0.086	2.287 ± 0.005	7.77 ± 0.75	0.095
Al	2.350 ± 0.005	6.73 ± 0.75	0.091	2.269 ± 0.005	6.68 ± 0.75	0.094
Ga	2.358 ± 0.005	6.83 ± 0.75	0.093	2.275 ± 0.005	6.40 ± 0.75	0.093
Sc	2.364 ± 0.005	7.77 ± 0.75	0.092	2.278 ± 0.005	7.47 ± 0.75	0.096
Zr	2.368 ± 0.005	8.47 ± 0.75	0.098	2.286 ± 0.005	6.98 ± 0.75	0.094
Hf	2.361 ± 0.005	7.89 ± 0.75	0.096	2.278 ± 0.005	6.96 ± 0.75	0.091

3.2. Eu^{3+} emission spectra

The Eu^{3+} emission spectra of the Zn, Al, Ga, Sc, Zr and Hf glasses are shown in figure 4. As can be seen from the figure, the $^5D_0 \rightarrow {}^7F_0$, $^5D_1 \rightarrow {}^7F_3$ and $^5D_0 \rightarrow {}^7F_1$ emission bands overlap each other. Thus the deconvolution of each band was necessary in order to obtain the peak position of $^5D_0 \rightarrow {}^7F_0$ emission and to calculate the ratio of the $^5D_0 \rightarrow {}^7F_2$ to $^5D_0 \rightarrow {}^7F_1$ emission intensities. The deconvolution was performed with a Gaussian-type function using a curve-fitting program of the least squares method. As an example, the deconvolution fitting performed for the Sc glass is shown in figure 5.

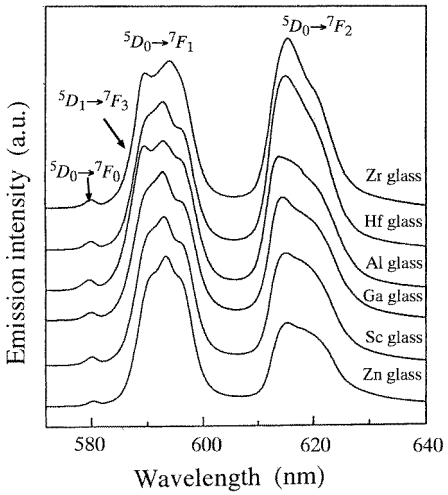

Figure 4. Eu^{3+} emission spectra of the Zn, Al, Ga, Sc, Zr and Hf glasses.

The peak position of $^5D_0 \rightarrow {}^7F_0$ emission and the ratio of the $^5D_0 \rightarrow {}^7F_2$ to $^5D_0 \rightarrow {}^7F_1$ emission intensities in the Zn, Al, Ga, Sc, Zr and Hf glasses are given in tables 2 and 3, respectively.

4. Discussion

The relationship between the Eu^{3+}–F^- interionic distance and the Er^{3+}–F^- interionic distance in the Zn, Al, Ga, Sc, Zr and Hf glasses is shown in figure 6, together with

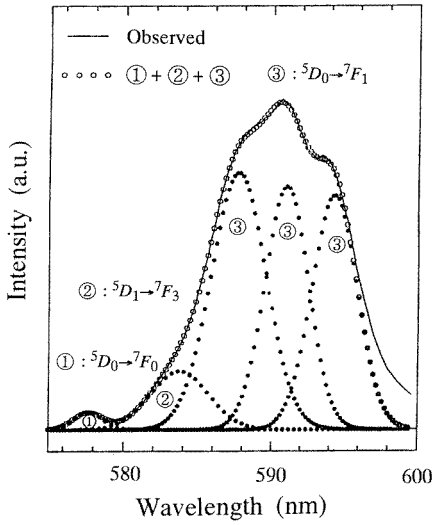

Figure 5. Deconvolution fitting of Eu^{3+} emission spectrum of the Sc glass.

Table 2. Peak position, ν_0, of $^5D_0 \rightarrow {}^7F_0$ emission in the Zn, Al, Ga, Sc, Zr and Hf glasses.

Glass	ν_0 (cm^{-1})
Zn	$17\,230 \pm 5$
Al	$17\,254 \pm 5$
Ga	$17\,245 \pm 5$
Sc	$17\,239 \pm 5$
Zr	$17\,241 \pm 5$
Hf	$17\,247 \pm 5$

Table 3. Intensity ratios of $^5D_0 \rightarrow {}^7F_2$ emission to $^5D_0 \rightarrow {}^7F_1$ emission, R, in the Zn, Al, Ga, Sc, Zr and Hf glasses.

Glass	R
Zn	0.70 ± 0.01
Al	0.97 ± 0.01
Ga	0.97 ± 0.01
Sc	0.90 ± 0.01
Zr	1.10 ± 0.01
Hf	1.25 ± 0.01

the experimental errors. The following three facts can be seen from the figure. Between the Eu^{3+}–F^- interionic distances and the Er^{3+}–F^- interionic distances there is a linear relationship with slope equal to about 1. The Eu^{3+}–F^- and Er^{3+}–F^- interionic distances are different with glass system, i.e. the Al glass has the shortest interionic distance and the Zn glass has the longest one. The Er^{3+}–F^- interionic distances are on the average 0.08 Å shorter than the Eu^{3+}–F^- interionic distances, corresponding to lanthanoid contraction in ionic radius. This difference in interionic distance leads to a difference in F^- coordination number, that is, the average F^- coordination number was 7.6 for Eu^{3+} and 7.1 for Er^{3+},

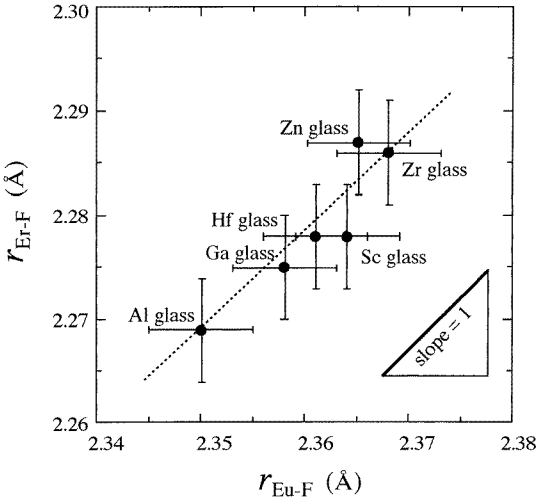

Figure 6. Relationship between Eu^{3+}–F^- interionic distances, r_{Eu-F}, and Er^{3+}–F^- interionic distances, r_{Er-F}, in the Zn, Al, Ga, Sc, Zr and Hf glasses.

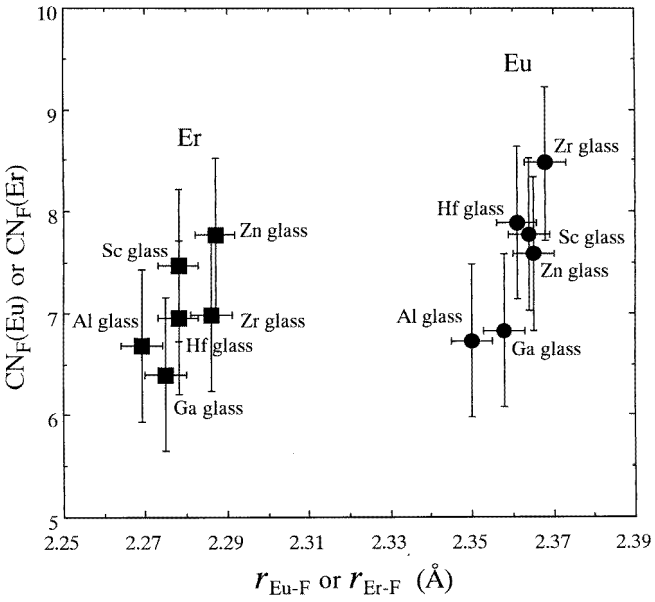

Figure 7. F^- coordination numbers of Eu^{3+} and Er^{3+}, $CN_F(Eu)$ and $CN_F(Er)$, plotted against the Eu^{3+}–F^- and Er^{3+}–F^- interionic distances, r_{Eu-F} and r_{Er-F}.

as shown in figure 7. The above facts lead to the conclusion that the F^- coordination environments around Eu^{3+} and Er^{3+} in each glass system are almost the same, except for slight differences due to lanthanoid contraction.

On the other hand, the Ln^{3+}–F^- interionic distances and the F^- coordination numbers around Ln^{3+} are significantly different with glass system, as can be seen from figures 6 and 7. This may be attributed to the following factor. The ionic field strengths, i.e. the ratios

of electric charge to ionic radius, of the Zn^{2+}, Al^{3+}, Ga^{3+}, Sc^{3+}, Zr^{4+} and Hf^{4+} ions are 2.26, 4.48, 3.95, 3.45, 4.08 and 4.12 $Å^{-1}$, respectively. On the other hand, the average F^- coordination numbers of the respective ions are roughly 6, 6, 6, 6, 8 and 8, respectively [14]. As a result, the positive charges which contribute to one of the coordinated F^- ions in the F^- coordination polyhedra of Zn^{2+}, Al^{3+}, Ga^{3+}, Sc^{3+}, Zr^{4+} and Hf^{4+} are 0.37, 0.74, 0.66, 0.575, 0.51 and 0.515 $Å^{-1}$, respectively. Thus the electrostatic attraction force increases in the order of the Zn^{2+}–F^-, Zr^{4+}–F^-, Hf^{4+}–F^-, Sc^{3+}–F^-, Ga^{3+}–F^- and Al^{3+}–F^- pairs. This suggests that the electron clouds of F^- ions are drawn toward these cations, consequently leading to interionic distances between the Eu^{3+}–F^- or Er^{3+}–F^- pair decreasing in that order.

In the Eu^{3+} emission spectra, the $^5D_0 \rightarrow {}^7F_0$ emission is not subject to crystal field splitting and is a transition between two non-degenerate levels. Both levels are displaced downward upon increasing Eu^{3+}-ligand interaction. The displacement of the upper, less shielded levels is smaller, and thus the $^5D_0 \rightarrow {}^7F_0$ transition occurs at shorter wavelengths, i.e. larger wavenumbers [15]. The $^5D_0 \rightarrow {}^7F_0$ emission bands observed for the Zn, Al, Ga, Sc, Zr and Hf glasses are plotted against the Eu^{3+}–F^- interionic distances in figure 8. It can be seen from the figure that glasses with shorter Eu^{3+}–F^- interionic distances give larger $^5D_0 \rightarrow {}^7F_0$ emission energies. This result indicates that the Eu^{3+}–F^- interionic distances, which were obtained by Eu EXAFS experiments, are reliable.

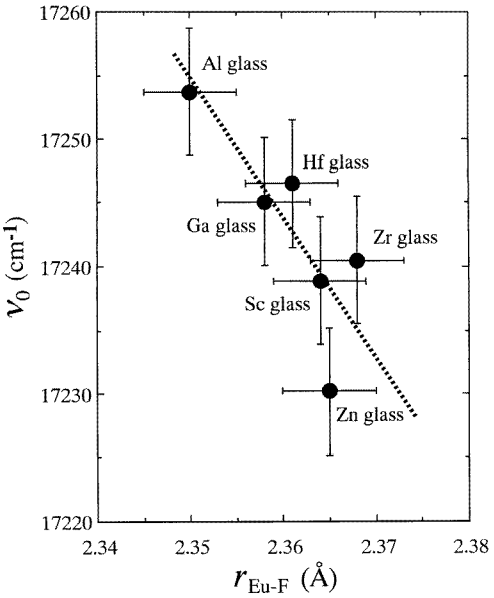

Figure 8. Relationship between Eu^{3+}–F^- interionic distances, r_{Eu-F}, and $^5D_0 \rightarrow {}^7F_0$ emission energies, ν_0, in the Zn, Al, Ga, Sc, Zr and Hf glasses.

Here the following fact also can be added. In the Eu^{3+} emission spectra the $^5D_0 \rightarrow {}^7F_2$ emission band is due to the electric-dipole transition, depending largely on the local symmetry of the coordination environment around Eu^{3+}, while the $^5D_0 \rightarrow {}^7F_1$ emission band is due to the magnetic-dipole transition, which is independent of local symmetry [16]. Therefore the ratio of the emission intensities of the $^5D_0 \rightarrow {}^7F_2$ to $^5D_0 \rightarrow {}^7F_1$ gives information about the degree of asymmetry in the F^- surroundings of the Eu^{3+} ion. As

can be seen from table 3, the ratios of the $^5D_0 \rightarrow {}^7F_2$ to $^5D_0 \rightarrow {}^7F_1$ emission intensities in the present glasses are in the order Zn glass < Sc glass < Al glass = Ga glass < Zr glass < Hf glass. The ratio values may be divided into three groups: (Zn glass), (Al, Ga and Sc glasses) and (Zr and Hf glasses), depending roughly on the electric charges of glass-network forming cations, Zn^{2+}, Al^{3+}, Ga^{3+}, Sc^{3+}, Zr^{4+} and Hf^{4+}. This occurs because, when the electric charge of the glass-network forming cation is smaller than that of Eu^{3+}, the Eu^{3+} ions can adopt the F^- coordination environment with higher symmetry. On the other hand, when the electric charge of the glass-network forming cation is larger than that of Eu^{3+}, the glass-network forming cation can adopt the F^- coordination environment with higher symmetry.

5. Conclusion

The F^- coordination environments around Eu^{3+} and Er^{3+} in MF_n–BaF_2–LnF_3 glass systems (M = Zn, Al, Ga, Sc, Zr or Hf; $n = 2$ for Zn, 3 for Al, Ga and Sc, 4 for Zr and Hf; Ln = Eu or Er) were examined by Eu and Er EXAFS spectroscopy and by Eu^{3+} emission spectroscopy. Glass compositions used are $55ZnF_2 \cdot 30BaF_2 \cdot 15LnF_3$, $45AlF_3 \cdot 30BaF_2 \cdot 25LnF_3$, $45GaF_3 \cdot 30BaF_2 \cdot 25LnF_3$, $45ScF_3 \cdot 40BaF_2 \cdot 15LnF_3$, $50ZrF_4 \cdot 30BaF_2 \cdot 20LnF_3$ and $50HfF_4 \cdot 30BaF_2 \cdot 20LnF_3$. The present experimental results clarified two facts. One is that the F^- coordination environments around Eu^{3+} and Er^{3+} significantly vary with the MF_n glass system. The other is that Er^{3+} and Eu^{3+} in the respective glasses have almost the same F^- coordination environments, though the Ln^{3+}–F^- interionic distance and the F^- coordination number of Ln^{3+} very slightly differ between Eu^{3+} and Er^{3+} due to lanthanoid contraction. The present experimental facts proved the validity of employing Eu^{3+} as a probe of Er^{3+} in order to obtain information about the physicochemical environments of Er^{3+} in Er^{3+} upconversion luminescence fluoride glasses.

Acknowledgment

The EXAFS measurements were performed under the approval of the Photon Factory Program Advisory Committee (PF-PAC proposal No 92-019).

References

[1] Quimby R S 1991 *Fluoride Glass Fiber Optics* (San Diego, CA: Academic)
[2] Takahashi M, Kanno R, Kawamoto Y, Tanabe S and Hirao K 1993 *Mater. Res. Bull.* **28** 557
[3] Chamarro M A and Cases R 1990 *J. Lumin.* **46** 59
[4] Yeh D C, Sibley W A, Suscavage M and Drexhage M G 1987 *J. Appl. Phys.* **62** 266
[5] Takahara K, Kanno R, Kawamoto Y, Tanabe S and Hirao K 1992 *Nippon Kagaku Kaishi* **1992** 103
[6] Tanabe S, Takahara K, Takahashi M and Kawamoto Y 1995 *J. Opt. Soc. Am.* B **12** 786
[7] Kawamoto Y, Kanno R, Yokota R, Takahashi M, Tanabe S and Hirao K 1993 *J. Solid State Chem.* **103** 334
[8] Takahashi M, Kanno R, Kawamoto Y, Tanabe S and Hirao K 1994 *J. Non-Cryst. Solids* **168** 137
[9] Poulain M, Poulain M and Lucas J 1973 *J. Solid State Chem.* **8** 132
[10] Teo B K 1986 *EXAFS: Basic Principle and Data Analysis* (Berlin: Springer)
[11] Maeda H 1987 *J. Phys. Soc. Japan* **56** 2777
[12] MaKale A G, Veal B W, Paulikas A P, Chan S K and Knapp G S 1988 *J. Am. Chem. Soc.* **1100** 3763
[13] Shannon R D 1976 *Acta Crystallogr.* A **32** 751
[14] Kawamoto Y, Kanno R, Kobayashi T and Takahashi M 1997 *Phys. Chem. Glasses* **38** 132
[15] Motegi N and Shionoya S 1973 *J. Lumin.* **8** 1
[16] Gallagher P K, Kurkjian C R and Bridenbaugh P M 1965 *Phys. Chem. Glasses* **6** 95